Analytical study of vertical external-cavity surface-emitting organic lasers

H. Rabbani-Haghighi, S. Forget, A. Siove, S. Chénais

Analytical study of Vertical External Cavity Surface-emitting Organic Lasers

H. Rabbani-Haghighi, S. Forget, A. Siove and S. Chénais

Laboratoire de Physique des Lasers, Université Paris 13 / CNRS, 99 avenue Jean-Baptiste Clément, 93430 Villetaneuse, France
E-mail: hadi.rabbani@univ-paris13.fr

Abstract

In this paper we report a detailed study of emission dynamics of an organic solid-state laser structure so-called VECSOL standing for Vertical External Cavity Surface-emitting Organic Laser recently developed in our group. An optical-optical efficiency of 43% and 6.3% were reported for a 4-mm-long cavity incorporating 18-µm-thick film of Poly (methyl methacrylate) (PMMA) doped with 1 wt% of Rhodamine 640 when pumped with 7-ns-long and 0.5-ns-long pulses respectively. In order to understand the difference seen in lasing efficiency as a function of different parameters such as cavity length or pump pulse duration, *Tang-Statz-deMars* cavity rate equations are used to model the emission behavior in a pulsed regime. Based on this model, conversion efficiency could be optimized practically to values as high as 57%. Furthermore, some characteristics of this laser architecture such as lasing lifetime (up to 140000 pulses at two times above lasing threshold), wavelength tuning (over 40 nm) and the system power scalability with potential operation up to mJ level are investigated.

1) Introduction

Organic semiconductor lasers based on polymers and small molecules have been an intense field of research in recent years [1-3]. This is mainly due to wide spectral tunability and simple processing techniques of organic materials (*e.g.* via spin coating or thermal evaporation) which has led to compact, tunable and inexpensive solid-state laser sources with potential applications in different fields such as spectroscopy [4, 5], bio/chemo sensing [6, 7] and short-haul data telecommunications via plastic optical fibers [8]. There are numerous reports of such devices under optical pumping in different laser configurations such as distributed feedback resonators [9], vertical microcavities [10, 11] and external-cavity resonators [12]. In the perspective of having compact organic laser sources which integrate the pump and the laser cavity in a small-volume device, there have been several achievements through indirect electrical pumping of organic solid-state lasers via Light Emitting Diodes [13] or nitride diode lasers [14, 15] by means of somehow sophisticated electronic circuitry systems for the pump source to make it operate in a pulsed regime. This indirect excitation approach has been chosen since realization of direct electrically-pumped organic semiconductor laser is hindered by several heavy constraints like low charge-carrier mobility of organic semiconductor materials as well as several loss mechanisms such as electrode losses and polaronic absorption [16-18]. Therefore, optically-pumped organic semiconductor lasers are of foremost importance.

Among several existing laser architectures for optically-pumped organic lasers, the external-cavity resonators are of great interest to provide efficient output power extraction possibility, excellent beam quality and power scalability. Nonetheless, in most cases the organic amplifying medium addressed in reports concerning this kind of laser architecture is prepared by complicated and long processes such as sol-gel [19] or radical polymerization [20] techniques which sometimes may take up to several days or weeks. Zavelani-Rossi *et al.* [21] has proposed an external cavity model based on spin-coated neat films of electroluminescent oligothiophenes. However based on this report regarding the cavity length (~ 6 µm) and the low output energy, it would rather be classified as a microcavity.

Recently, we have reported on a very simply-built external cavity organic laser, so-called Vertical External Cavity Surface-emitting Organic Laser (VECSOL) which has brought together a combination of high output powers, excellent efficiency as well as good beam quality in a single device [22]. The laser architecture was basically inspired from the traditional inorganic Vertical External Cavity

Surface Emitting Laser (VECSEL) and consisted of a highly reflective dielectric plane mirror (R> 99.5% within the range of 600-660 nm) onto which an amorphous film (~ 18-µm-thick) of Poly (methyl methacrylate) (PMMA) doped with 1 wt% of Rhodamine 640 was directly deposited through spin coating process. A meniscus output coupler of 98% reflectivity within the range of 600-680 nm closed the cavity (Figure 1.a). The whole set up was end-pumped by a frequency-doubled Nd:YAG laser at 532 nm. In this configuration and for a typical case of 4-mm-long laser cavity, a diffraction-limited laser emission ($M^2 = 1$) with an optical-optical efficiency as high as 43% and 6.3% were obtained for 7-ns-long and 0.5-ns-long pump pulses respectively, under 10 Hz repetition rate excitation regime. Lasing was observed for cavity lengths up to 60 mm in case of pumping with 7-ns-long pulses whereas this was limited to 10 mm for 0.5-ns-long pump pulses. A noticeable feature of the VECSOL architecture is its open cavity, allowing intracavity frequency doubling and consequently UV emission from an organic thin-film device [23].

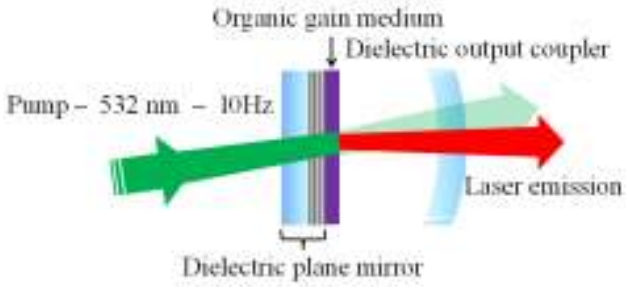

Figure 1.a
Experimental setup of the VECSOL cavity under optical pumping

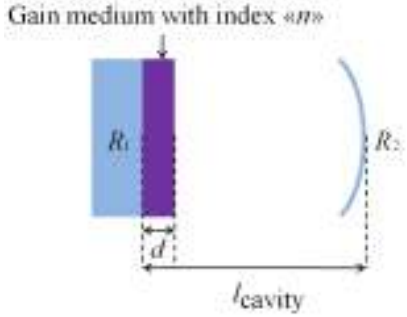

Figure 1.b
Schematic representation of different cavity parameters (see text)

In the present article we perform a detailed study of the VECSOL performance through experiment followed by theoretical modeling via application of the *Tang-Statz-deMars* rate equations in a pulsed regime [24]. This may help to understand how variations of different parameters such as cavity length or pump pulse duration would affect emission behaviors. Furthermore, VECSOL performance optimization is carried out by inspecting among different resonator elements and then wavelength tuning, photostability and power scalability are demonstrated in the last part.

2) Theoretical background

Consider an amplifying gain medium (index n) of thickness "d" and a pumped region of cross sectional area "S" inserted between two mirrors with R_1 and R_2 reflectivities to build a laser cavity with an optical length of $L=(n-1)d+l_{cavity}$ where l_{cavity} is the physical length of the cavity (Figure 1.b). The cavity rate equations over the $S.L$ volume (mode volume) showing the evolution of the output laser intensity and the population inversion would be the following[24]:

$$\frac{dI}{dt} = \frac{1}{\tau_{cav}}\left[\frac{\Delta N}{\Delta N_{th}}\left(I + \frac{c}{SL}\right) - I\right] \quad (1)$$

$$\frac{d\Delta N}{dt} = \frac{1}{\tau_{eff}}\left[\Delta N_0 - \Delta N\left(1 + \frac{I}{I_{sat}}\right)\right] \quad (2)$$

where I is the laser intensity in photonic unit (photons/s/m^2) and c is denoting the speed of light. $\Delta N=N_2-N_1$ is defined as the population inversion (m^{-3}) in a four-level system between the low excited-state and one of the ground-state vibronic levels, depending on the emission wavelength. ΔN_{th} is the population inversion at threshold.
τ_{cav} is the photon life time inside the cavity and is derived as

$$\tau_{cav} = \frac{-2L}{c.Ln[R_1 R_2 (1-T_i)^2]} \quad (3)$$

with T_i representing the single-pass cavity passive losses due to gain medium absorption, diffusion or mirror scattering.
τ_{eff} is described as the effective non-saturated excited-state lifetime as it determines the excited-state filling time when I=0 ;

$$\tau_{eff} = \frac{\tau}{1+\frac{I_p}{I_{p_{sat}}}} \quad (4)$$

with τ, I_p and $I_{p_{sat}}$ symbolizing the singlet excited-state radiative lifetime, the pump intensity (assumed to be constant during the pump pulse duration) and saturation pump intensity respectively. I_{sat} is defined as the laser saturation intensity and ΔN_0 stands for the non-saturated population inversion with N showing the density of molecules in the active region;

$$\Delta N_0 = \frac{N\frac{I_p}{I_{p_{sat}}}}{1+\frac{I_p}{I_{p_{sat}}}} \quad (5)$$

It should be mentioned that the theory which is introduced here to be used for the following simulations, holds for a four-level system operating in a single-mode regime. It does not take into account the existence of a microcavity formed by the organic film which was shown to control the emitted spectrum. It also neglects intramolecular as well as intermolecular phenomena that occur once the molecules are in the excited state such as quenching or triplet state absorption which make this system more complex than a true four-level system. In the following part we investigate the observed VECSOL emission characteristic behavior and then explain this behavior through some simulations.

3) VECSOL dynamics analysis

Before starting the analysis, it should be reminded that a rectangular-shape pump profile is used for the modelling purpose. Based on simulations which apply the cavity rate equations to a typical case of 4-mm-long VECSOL with R_1 =99.5% and R_2 =98% and an amplifying gain medium of ~18-µm-thick, in case of exciting the cavity with 7-ns-long pulses and 10 Hz repetition rate, the laser oscillation builds up in a rather short time with respect to the pump pulse duration (Figure.2). In this case the steady state is reached before the pulse finishes and would last till the end of the pulse which causes an efficient extraction of the pump energy during 7 ns and thus very high conversion efficiency. In case of pumping the cavity with 0.5-ns-long pulses and for the same cavity length, the population inversion is also created in a fraction of a ns after excitation but the laser field does not have enough time to exceed the cavity losses within the pulse time period. In this case the created population inversion lasts for ~ 0.25 ns after the end of the pump pulse and before the beginning of laser oscillation buildup since the excited-state life time (7.5 ns) [25] is longer than the pulse duration. When the laser oscillation starts, the pump pulse has already terminated and the population inversion has a descending trend to zero and the steady sate will never be reached. Therefore, the conversion efficiency would be low in this case even if a rather high output peak power could be obtained. A comparison between the experimental conversion efficiencies (43% and 6.3% corresponding to 7-ns-long and 0.5-ns-long pump pulses respectively) confirms the above-described analysis. Theoretical calculation of the efficiency values follows the same trend as a function of pump pulse duration but with a difference (30% instead of 43% and 2.5% instead of 6.3%) which is likely to be due to model limits introduced previously and above all, neglect of the existing microcavity for the simulations.
The pulse-duration-dependant VECSOL behavior can also be justified numerically by estimating the number of absorption/emission cycles that each molecule experiences within the pump pulse duration. In the case of 7-ns-long pulses, the output energy of 6 µJ obtained from an excited region containing ~ 3.10^{12} molecules would mean an average number of 6 photons emitted per molecule and per pulse.

This can be interpreted as the case where each molecule undergoes an average of 6 absorption/emission cycles during 7 ns. When the pulse duration is 0.5 ns, the output energy of 0.7 µJ corresponds to an average photon number of 0.7 per molecule during the pulse time. This validates the conclusion taken from Figure.2 that steady state is reached for 7-ns-long pulses whereas it is not the case for 0.5-ns-long pump pulses.

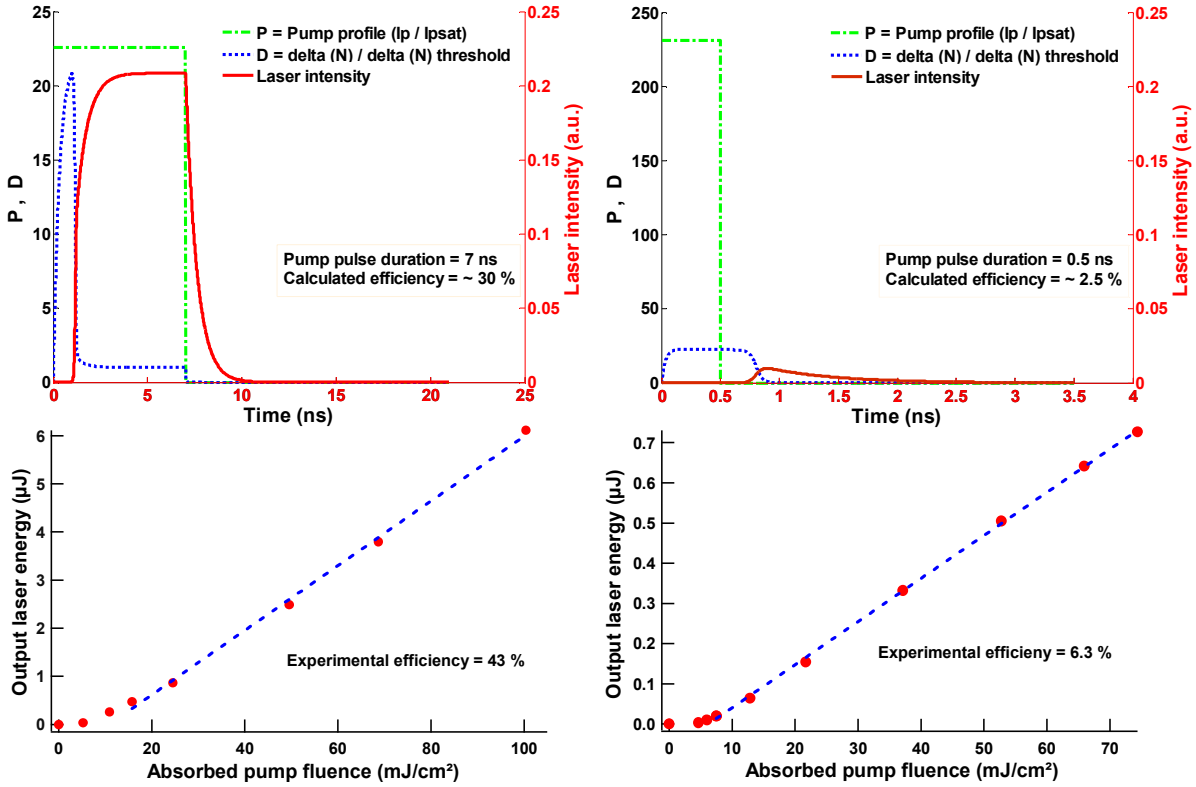

Figure 2

Oscillation buildup time simulations for 7-ns-long pump pulse (left) and 0.5-ns-long pump pulse (right) and below are the corresponding experimental efficiency curves for each case. In practice as well as for the modeling, the cavity is 4-mm-long. The only fitting parameter for the simulations is the roundtrip passive loss which is considered 2%.

Consequently, as the pump pulse duration has a dramatic effect on the laser efficiency, similarly the cavity length is an important parameter as it directly intervenes in the oscillation buildup time for a given pump pulse duration. This behavior is theoretically modeled for pump pulses of 7 ns and 0.5 ns and for sake of comparison each time for two different cases of Gaussian and rectangular pump profiles (Figure.3). In both cases the VECSOL energy drops down as the cavity length increases. The collapse of output energy by lengthening the cavity could be explained in a similar way as shortening the pump pulse duration by an increase of the oscillation buildup time with respect to pump duration and therefore a decrease of the efficiency.

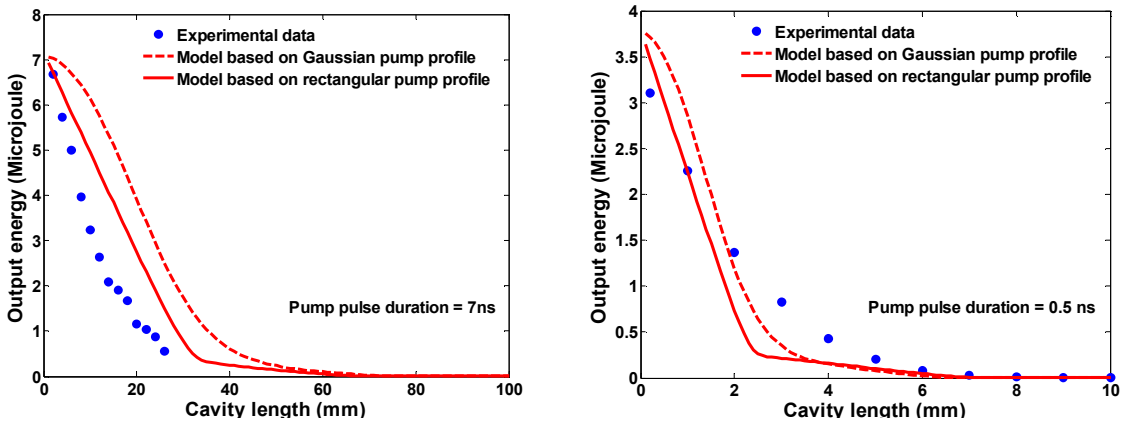

Figure 3

VECSOL output energy dependency on cavity length for two different pump pulse durations (7 ns and 0.5 ns). The only fitting parameter is the roundtrip passive loss which is considered 2%

4) VECSOL performance optimization

These results can now serve as a basis to find out the optimum parameters for lasing action in order to achieve the highest possible output energy. One of the criteria which would help to achieve the best lasing efficiency is to look for the optimum output coupler. This is due to the fact that one might expect an increase in the output signal intensity and therefore the efficiency by reducing the mirror reflectivity but this would also shorten the intra-cavity photon lifetime followed by a decrease in the output energy. In this case there is compromise that must be respected in choosing the output coupler in order to have the best lasing performance. Based on the previous simulations, the highest conversion efficiency is obtained for an output coupler of 95% reflectivity. This is also shown experimentally for four different available output couplers (80%, 90%, 95% and 98%) and a cavity length fixed to 10 mm (Figure.4). As it is seen, the experimental data and the simulation are in good agreement. From these data, the output coupler of 98% reflectivity used in ref [22] was replaced by the optimized output coupler of 95% reflectivity and the VECSOL conversion efficiency was improved from 43% to 57% for a cavity length of 1mm when excited with pulses of 7-ns-long at 10 Hz repetition rate (Figure.5).

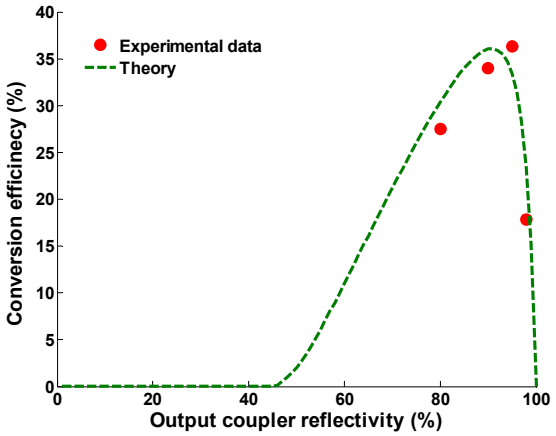

Figure 4
Filled circles are the experimental data obtained for 10-mm-long cavity length, 18-µm-thick gain medium and an incident pump fluence of 100 mJ/cm^2. The dashed line is a model showing the evolution of the conversion efficiency by output coupler reflectivity variation in a range from zero to hundred. The only fitting parameter is the roundtrip cavity loss which is set to 2%.

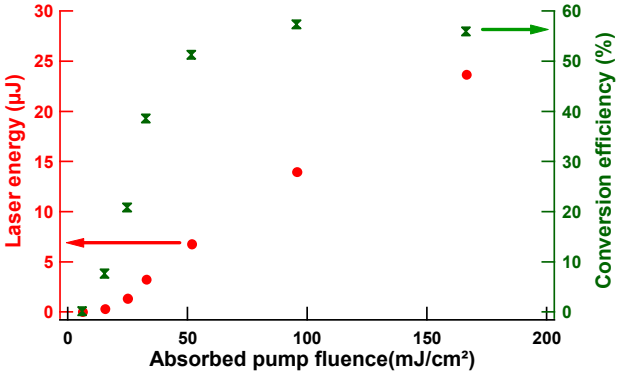

Figure 5
(Left axis) Laser energy, (Right axis) conversion efficiency as a function of the absorbed pump fluence for an optimum output coupler of 95% reflectivity, 1-mm-long cavity and 18-µm-thick gain medium. The small efficiency drop seen at the end could be due to degradation issues at this excitation intensity.

5) VECSOL emission characterization

VECSOL emission spectrum is a result of a Fabry-Perot etalon formed by the organic gain medium which is coupled to the external cavity. It consists of several peaks, with 7.8 nm distance between the peaks which corresponds to the free spectral range of the ~ 18-µm-thick etalon. ($\Delta\lambda = \frac{\lambda^2}{2nl}$ with n the refractive index of the medium, l the film thickness and λ the emission wavelength) (Figure.6). Each of these peaks is containing the external cavity modes with a free spectral range that would be decreased as the cavity length increases. The free spectral range corresponding to a 1-mm-long cavity is a fraction of nm. Therefore the external cavity modes are not resolved with the resolution (0.5 nm) of the spectrometer (Spex 270M) at disposal. By modulating the rotation speed during the spin coating process and by using lower density PMMA it is possible to reduce the film thickness in order to have only one mode of the Fabry-Perot etalon under the gain spectral region of the organic material. Single-peak laser operation was observed for 2.35-µm-thick film which still contains the external cavity modes inside of it (Figure.7).

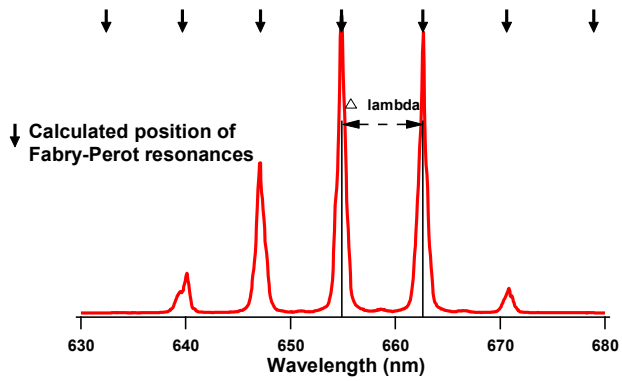

Figure 6
Typical VECSOL emission spectrum of a 18-µm-thick gain medium. Small arrows pointing down are indicating the position of Fabry-Perot peaks obtained by simulation.

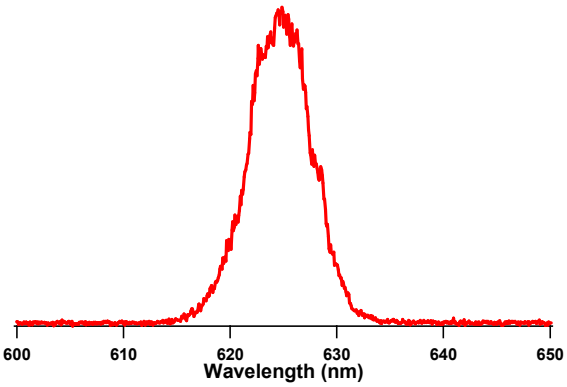

Figure 7
Single-mode laser operation obtained for a 2.35-µm-thick film. This peak comprises several external cavity modes but the observation is limited by spectrometer resolution. However the external cavity mode competition can still be seen on the top of this peak.

6) Tunability

Certainly, among the most interesting features of the VECSOL emission is the wavelength tuning achieved thanks to clever use of film thickness variation obtained via spin coating by going toward the sample edge. The intrinsic characteristic of the films realized through spin coating is a flat zone in the middle and then a gradual increase as it goes toward the edge. This fact is verified experimentally by measuring the deposited film thickness with a profilometer from the center to the edge on a standard-size plane mirror (diameter = 25.4 mm) (Figure.8). For the purpose of wavelength tuning demonstration, a sample 2.35-µm-thick sample was prepared to operate in single-mode regime. When the coated plane mirror moved transversely to the pump beam, as it approached to the edge, a tuning range of around $\Delta\lambda$ = 40 nm (from 615 nm to 655 nm) could be obtained, limited by the gain spectrum and the mirror reflectivities (Figure.9).

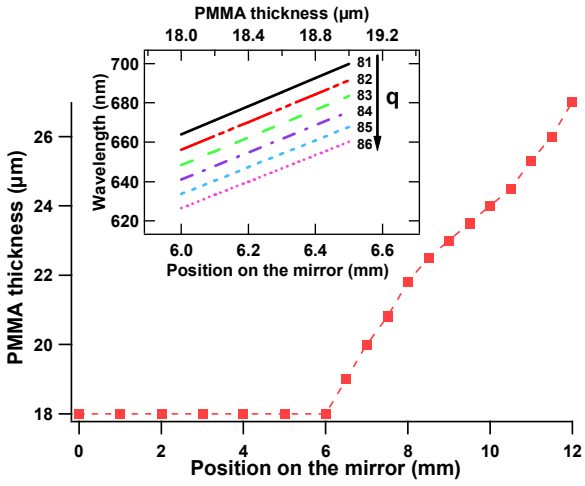

Figure 8
PMMA thickness variation as it goes toward the sample edge for a 18-µm-thick film. The inset is the simulation showing the peak wavelengths in a Fabry-Perot when the film thickness varies as a function of the position on the mirror. q numbers are representing the Fabry-Perot resonance modes residing within the Rhodamine 640 gain region.

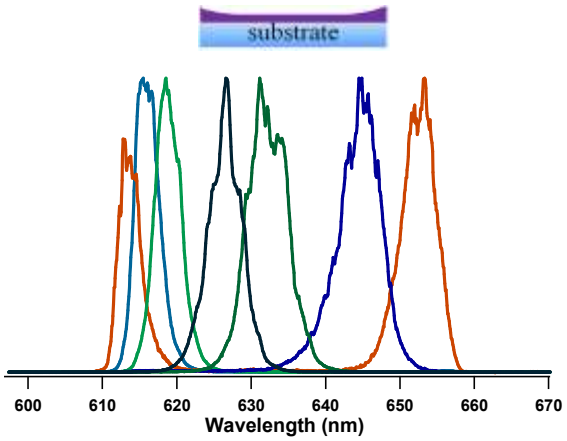

Figure 9
Tunability obtained over 40 nm from 615 nm to 655 nm for 2.35-µm-thick film due to film thickness variation. (Inset) schematic representation of film thickness variation by going toward sample edges.

7) Laser emission lifetime and power scalability

In terms of stability, the VECSOL was irradiated at 10 Hz repetition rate by two pump sources with 7 ns and 0.5 ns pulse durations. As it is seen in Figure.10 the laser energy reduced to half of its initial value after 140000 pulses in case of pumping with 7-ns-long pump pulses whereas this happened after 5000 pulses when the VECSOL is pumped by 0.5-ns-long pulses and an absorbed pump fluence of ~ 15 mJ/cm^2 in both cases. The higher degradation rate in the case of pumping with 0.5-ns-long pulses might be mainly due to higher absolute pump power which is ~ 20 times higher in this case. The lasing lifetimes are comparable (or even far better, given the high pump fluence used in our case) to values reported in the literature for organic thin film devices [26].

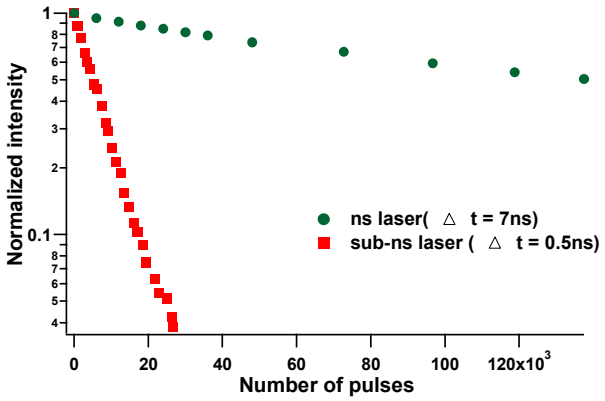

Figure 10

VECSOL normalized intensity versus the number of pumps pulses for two different pump pulse durations of 0.5 ns and 7 ns and a pump fluence of ~ 15 mJ/cm^2 in both cases.

Another interesting feature of the VECSOL is the power scalability or in other words the possibility of increasing the output power or energy without decreasing the laser lifetime. As an example, we were interested to show that the output energy is doubled when the VECSOL is pumped by incident energy twice higher, while the incident pump fluence and consequently the degradation rate are kept constant. For this purpose, we started the experiment with an output coupler of 98% reflectivity with 50 mm radius of curvature. The TEM_{00} fundamental mode waist radius corresponding to this curvature is 52 µm. Therefore, a pump waist radius of 60 µm was chosen in order to have only a predominant pump area over the TEM_{00} fundamental cavity mode and not the higher order transverse modes. In another case, the pump waist size of 85µm was chosen in order to enlarge the pump surface area by a factor of two. So the output coupler was replaced with an output coupler of 98% reflectivity and 200 mm radius of curvature to match this pump size and the fundamental TEM_{00} cavity mode (having in this case 75 µm waist size) together. The experimental results depicted in Figure.11 show identical degradation rates in accordance with our expectation for an incident pump fluence of 20 mJ/cm^2 which is roughly two times above lasing threshold in the case of 7-ns-long pump pulses.

It would be also useful to estimate the maximum attainable output energy of the VECSOL at the same pump fluence with a maximum pump beam diameter of 4 mm for example (for higher diameters, the beam spatial quality is likely to be disturbed by thermal effects) and a relevant output coupler that could match this pump beam size to TEM_{00} fundamental mode. In this condition, output energy of ~ 1 mJ would be achievable while preserving a low degradation rate.

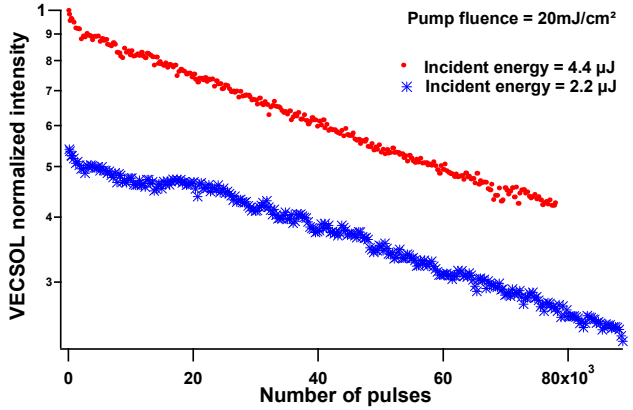

Figure 11

VECSOL power scaling demonstration for two typical incident energies

8) Conclusion

In conclusion we have explored through simulations and experiments, the VECSOL emission behavior (based on film of PMMA doped by 1 wt% of Rhodamine 640) in terms of lasing efficiency when the cavity length or the pump pulse duration was varied (7 ns and 0.5 ns). We observed that higher laser efficiency was directly related to longer pump pulse durations or similarly shorter cavity lengths due to shorter oscillation buildup time with respect to pump pulse duration. The realized simulations paved the way to improve VECSOL lasing efficiency to values as high as 57% by utilizing the optimum output coupler. The spectrum was controlled by the Fabry-Perot and a single-peak lasing operation could be achieved by reducing gain medium thickness to 2.35 μm. Wavelength tuning over 40 nm (615 nm-655 nm) was obtained thanks to thickness variation of the gain medium realized by the spin coating process. In terms of photostability, we demonstrated half lasing lifetime after 140000 pulses in normal condition when the VECSOL was pumped by 7-ns-long pulses. Finally, power scalability was an added value feature of the VECSOL architecture that will open the way toward high-energy organic lasers based on thin films.

The authors are grateful to Manal Yewakim for valuable assistance on the film thickness measurements, and the French National Research Agency (ANR, Young researchers program, grant # 07JCJC0029), for financial support.

References

1. N. Tessler, Adv. Mater. **11**, 363 (1999)
2. M.D. McGehee and Heeger A.J., Adv. Mater. **12**, 1655 (2000)
3. I.D.W. Samuel and Turnbull G.A., Chemical Reviews. **107**, 1272 (2007)
4. T. Woggon, Klinkhammer S., and Lemmer U., Applied Physics B-Lasers And Optics. **99**, 47 (2010)
5. Y. Oki, et al., Opt. Rev. **12**, 301 (2005)
6. M. Lu, et al., Applied Physics Letters. **93** (2008)
7. Y. Yang, Turnbull G.A., and Samuel I.D.W., Advanced Functional Materials. **20**, 2093
8. K. Kuriki, et al., Applied Physics Letters. **77**, 331 (2000)
9. H. Rabbani-Haghighi, et al., Applied Physics Letters. **95** (2009)
10. N. Tessler, Denton G.J., and Friend R.H., Nature. **382**, 695 (1996)
11. L. Persano, et al., Applied Physics Letters. **88** (2006)
12. I. Garcia-Moreno, et al., Advanced Functional Materials. **19**, 2547 (2009)
13. Y. Yang, Turnbull G.A., and Samuel I.D.W., Applied Physics Letters. **92** (2008)
14. T. Riedl, et al., Applied Physics Letters. **88** (2006)
15. H. Sakata and Takeuchi H., Applied Physics Letters. **92** (2008)
16. M. Reufer, et al., Applied Physics Letters. **84**, 3262 (2004)
17. T. Rabe, et al., Physical Review Letters. **102** (2009)
18. B.K. Yap, et al., Nature Materials. **7**, 376 (2008)
19. W.T. Hu, et al., Appl. Optics. **36**, 579 (1997)
20. A. Costela, et al., Applied Physics B-Lasers And Optics. **76**, 365 (2003)
21. M. Zavelani-Rossi, et al., Synthetic Metals. **139**, 901 (2003)
22. H. Rabbani-Haghighi, et al., Opt. Lett. **35**, 1968 (2010)
23. S. Forget, et al., Applied Physics Letters. **in press** (2011)
24. O. Svelto, *Principles of Lasers*. 5th edn. (Springer Science, 2010)
25. M.C. Ramon, et al., Journal Of Applied Physics. **97** (2005)
26. V. Navarro-Fuster, et al., Applied Physics Letters. **97**